

Magnetic states and reorientation transitions in antiferromagnetic superlattices

U. K. Rößler* and A. N. Bogdanov†

Leibniz-Institut für Festkörper- und Werkstofforschung Dresden, Postfach 270116, D-01171 Dresden, Germany

(Received 12 November 2003; published 11 March 2004)

Equilibrium spin configurations and their stability limits have been calculated for models of magnetic superlattices with a finite number of thin ferromagnetic layers coupled antiferromagnetically through spacers. Depending on values of applied magnetic field and uniaxial anisotropy, the system assumes collinear (antiferromagnetic, ferromagnetic, various “ferrimagnetic”) phases, or spatially inhomogeneous (symmetric spin-flop phase and asymmetric, *canted* and *twisted*, phases) via series of field induced continuous and discontinuous transitions. Contrary to semi-infinite systems a surface phase transition, so-called “surface spin flop,” does not occur in the models with a finite number of layers. It is shown that “discrete jumps” observed in some Fe/Cr superlattices and interpreted as “surface spin flop” transition are first-order “volume” transitions between different canted phases. Depending on the system these collinear and canted phases can co-exist as metastable states in broad ranges of the magnetic fields, which may cause severe hysteresis. The results explain magnetization processes in recent experiments on antiferromagnetic Fe/Cr and Co/Ru superlattices.

DOI: 10.1103/PhysRevB.69.094405

PACS number(s): 75.70.-i, 75.10.-b, 75.30.Kz, 75.50.Ee

Antiferromagnetic coupling in magnetic multilayers mediated by spacer layers and giant magnetoresistance are two related phenomena that have created the basis for applications of antiferromagnetic superlattices as Fe/Cr, Co/Cu, or Co/Ru.¹ Multilayer stacks with antiferromagnetic interlayer couplings are widely used in spin valves as *synthetic antiferromagnets*, in various other spinelectronics devices, and they are considered as promising recording media.² High quality multilayer stacks, such as Co/Ru,³ Fe/Cr(211),⁴ or Fe/Cr(001),⁵ can be considered as “artificial” nanoscale antiferromagnets. They provide experimental models for the magnetic properties of confined antiferromagnets under influence of surface effects. Hence, both for applications and from a fundamental point of view, such systems are of great importance and attract much interest in modern nanomagnetism.^{5–10}

In the last years, efforts based on experimental investigations,^{4–9} and theoretical studies^{4,10} to understand ground states and the transitions under magnetic fields in such multilayers resulted in a controversy around the problem of the so-called “surface spin flop.” This problem can be traced back to Mills’ theory¹¹ which predicted that in uniaxial antiferromagnets spins near the surfaces rotate into the flopped state at a field reduced by a factor of $\sqrt{2}$ compared to the bulk spin-flop field. In an increasing magnetic field such localized surface states spread into the depth of the sample.¹¹ In Ref. 4, the authors claimed to observe these surface states in Fe/Cr superlattices and supported their experimental results by numerical calculations. Subsequent theoretical studies (mostly based on numerical simulations within simplified discretized models¹¹) led to conflicting conclusions on the evolution of magnetic states in these systems.¹⁰ Finally, recent experimental investigations obtained different scenarios for reorientational transitions in Fe/Cr^{7–9} and Co/Ru⁶ multilayer systems.

This study provides a comprehensive analysis within the standard theory of phase transitions to determine all (one-dimensional) spin configurations and their stability limits for models of antiferromagnetic superlattices. Our results ex-

plain the diversity of experimentally observed effects in different antiferromagnetic multilayer systems.^{4–9} It is shown that the magnetization processes observed in Refs. 4 and 7 and interpreted as a manifestation of the “surface spin-flop transitions,” are a succession of first-order phase transitions between asymmetric inhomogeneous phases. Such transitions occur only in a certain range of uniaxial anisotropy. In the major parts of the *magnetic field vs uniaxial anisotropy* phase diagram the antiferromagnetic phase undergoes discontinuous transitions either into an inhomogeneous spin-flop phase (low anisotropy) or into ferrimagnetic collinear phases (high anisotropy).

The energy of a superlattice with N coupled ferromagnetic layers can be modeled by

$$W = \sum_{i=1}^{N-1} [J_i \mathbf{m}_i \cdot \mathbf{m}_{i+1} + \tilde{J}_i (\mathbf{m}_i \cdot \mathbf{m}_{i+1})^2] - \mathbf{H} \cdot \sum_{i=1}^N \mathbf{m}_i - \frac{1}{2} \sum_{i=1}^N K_i (\mathbf{m}_i \cdot \mathbf{n})^2 - \sum_{i=1}^{N-1} K'_i (\mathbf{m}_i \cdot \mathbf{n})(\mathbf{m}_{i+1} \cdot \mathbf{n}), \quad (1)$$

where the first two sums describe bilinear (J_i) and biquadratic (\tilde{J}_i) exchange interactions; K_i and K'_i are constants of uniaxial anisotropy, and \mathbf{H} is an applied magnetic field. Models of type (1) are commonly used to analyze magnetization processes in nanoscale magnetic multilayers systems^{4,5,7,8,12} and other superlattices.¹² The material constants in Eq. (1) are averaged effective parameters for one multilayer period, which may be internally inhomogeneous.^{13–15} Thermal fluctuations would become important only near to the Curie temperature, where the modulus of the magnetizations \mathbf{m}_i should be included as internal variables of the system. Thus, the model describes reorientational processes for fixed temperatures in the whole range of the ferromagnetically ordered state.

The antiferromagnetic superlattices considered in our analysis are composed of few tens of identical magnetic/spacer bilayers with fully compensated magnetization,^{3–9}

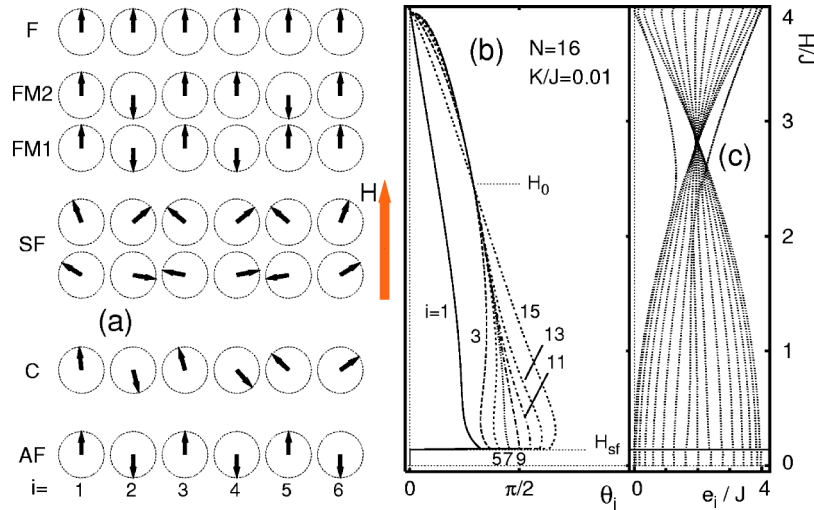


FIG. 1. (a) States in antiferromagnetic superlattices (example $N=6$) with increasing field: F ferromagnetic; FM1/2 ferrimagnetic collinear—such phases may be energetically degenerate, but they own different (meta-)stability limits; SF spin-flop states; C asymmetric-canted; AF antiferromagnetic). Example of evolution of state with field H for Mills model in low anisotropy case: (b) rotation angles θ_i (i odd) against easy axis $\mathbf{n} \parallel$ field \mathbf{H} (for i even $\theta_i = -\theta_{N-i+1}$). Phases of type C and FM1/2 may occur only at intermediate and higher anisotropy. (c) corresponding resonance spectrum.

i.e., systems with *even* number of ferromagnetic layers. To simplify the discussion, we assume that induced interactions in such systems maintain mirror symmetry about the center of the layer stack, i.e., $J_i = J_{N-i}$, $K_i = K_{N+1-i}$, etc. in the energy (1). Usually demagnetization fields confine the magnetization vectors \mathbf{m}_i to the layer plane, and their orientation within this plane can be described by their angles θ_i with the “easy axis” \mathbf{n} . Thus the problem of the magnetic states for the model (1) is reduced to optimization of the function $W(\theta_1, \theta_2, \dots, \theta_N)$. We assume that values of the magnetic parameters are such that the energy (1) yields a *collinear antiferromagnetic* (AF) phase as ground state in zero field, i.e., \mathbf{m}_i are directed along the easy axis \mathbf{n} and antiparallel in adjacent layers. Next, we consider the evolution of states with a magnetic field along the easy axis \mathbf{n} .

In the case of weak anisotropy ($\bar{J}_i \equiv J_i - 2\bar{J}_i \gg K_i, K'_i$) the applied field stabilizes a *spin-flop* (SF) phase with symmetric ($\theta_i = -\theta_{N-i+1}$) deviations of \mathbf{m}_i from the easy axis [Fig. 1(a)]. Contrary to spin-flop phases in bulk antiferromagnets, this SF phase is spatially inhomogeneous. At low fields the solutions for the SF phase are given by a set of linear equations $\bar{J}_{2j-1}(\pi - \theta_{2j-1} + \theta_{2j}) = H$, $\theta_{2j} - \theta_{2j+1} = 0$ ($j = 1, 2, \dots, l$, $l = N/4$ for systems with $N = 4n$ or $l = (N+2)/4$ for $N = 4n+2$, $n = 0, 1, \dots$). These solutions describe small deviations of the magnetization vectors, $|\theta_i - \pi/2| \ll 1$, from the directions perpendicular to the easy axis [Fig. 1(a)]. Towards top and bottom layer $i = 1$ or N in the stack, the deviations increase. For example, for $N = 10$ the solutions read $\theta_5 = \pi/2 - H/(2\bar{J}_5)$, $\theta_4 = \theta_5 - \pi$, $\theta_3 = \theta_5 - H/\bar{J}_3$, $\theta_2 = \theta_3 - \pi$, $\theta_1 = \theta_3 - H/\bar{J}_1$. The properties of these solutions and other particular magnetic configurations of the model (1) arise essentially due to *cut exchange bonds at the boundary layers*. This is different from surface-induced changes for magnetic states of other nanoscale systems. In ferromagnetic nanostructures, as in nanosized layers

of antiferromagnetic materials, noncollinear and/or twisted configurations are caused by particular surface-related anisotropy and exchange contributions due to modified (relativistic) spin-orbit effects near surfaces (as discussed, e.g., in Refs. 15,16). The simplified variant of the energy (1) with $J_i = J$, $K_i = K$, $\bar{J}_i = K'_i = 0$ embodies this cutting of bonds as the only surface effect and allows to investigate this effect separately from other surface-induced forces. This model, introduced by Mills as a semi-infinite model,¹¹ was later investigated in different cases also for finite systems.^{4,10} However, in spite of rather sophisticated methods used in these previous studies, the magnetic properties described by the model (called here *Mills model*) have remained elusive. Transitions and stability lines for the collinear phases can be calculated analytically, but the main body of our results have been obtained by numerical methods. We could investigate in detail systems up to $N=20$ (and some aspects of larger systems) using a combination of following methods. (i) Search for energy minima using of the order 1000 random starting states for a dense mesh of points in the phase diagram, (ii) an efficient conjugate gradient minimization¹⁷ to solve the coupled equations for equilibria $\{\partial W/\partial \theta_i = 0\}_{i=1 \dots N}$, (iii) calculation of stability limits from the evolution of the smallest eigenvalue $e_0(H, K)$ of the stability matrix $(\partial^2 W/\partial \theta_i \partial \theta_j)$, $i, j = 1 \dots N$ under changing anisotropy constant K and the applied magnetic field. The eigenvalue spectrum $\{e_i\}$ [see example in Fig. 1(c)] is related to magnetic resonances with moments precessing in the layer plane, viz $\mathbf{k} = 0$ spin waves. Instabilities are signaled by softening of these modes. The basic magnetic configurations are expounded below.

(i) Evolution of the *inhomogeneous* SF phases is given in Fig. 1. At low fields, due to the dominating role of the exchange interactions favoring antiparallel ordering of the magnetizations in adjacent layers, some of the “sublattices”

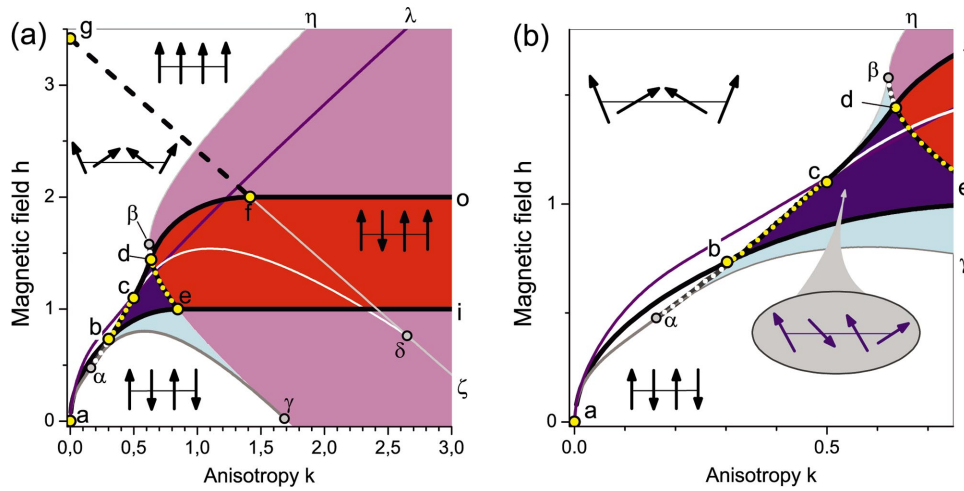


FIG. 2. (Color) Phase-diagram for Mills model with $N=4$: (a) overview (b) details at low anisotropy (in this region critical lines have been shifted for clarity). Full black lines are first order transitions between equilibrium states; continuous transitions are dashed and dotted. Equilibrium states: antiferromagnetic below $a-b-e-i$ line (AF); (red) area $o-d-e-i$ collinear “ferrimagnetic” (FM); area $a-b-d-f-g$ symmetric spin-flop phase (SF); (blue) area $b-e-d-c$ noncollinear asymmetric (C); above line $g-f-o$ ferromagnetic phase (F). Greek letters: critical points at boundaries of metastable states. Metastable states corresponding to FM exist in the region (magenta) right of line $\eta-\beta-d-e-\gamma$ and for C in the two regions $\alpha-b-e-\gamma-\alpha$ and $c-\beta-d-c$ (light blue), respectively. Further stability limits: for SF $a-\alpha-b-c$ and $c-\delta$ (white) $\delta-f-g$; for AF $a-\lambda$ (violet); for F $g-f-\delta-\zeta$.

have to rotate against the applied field. At sufficiently strong fields the sense of rotation for these sublattices is reversed [Fig. 1(b)]. Near saturation, the SF phase has only positive projections of the magnetization on the direction of the magnetic field which decreases towards the center similar to spin configurations described in Ref. 18. There is a special field (independent of N) where all inner sublattices have the same projection on the field direction [$\theta_i = (-1)^{i+1} \theta_0, i$

$= 2, 3 \dots N - 1$] [Fig. 1(b)]. The parameters of this “knot” point are determined from the equations $H_0/J = (4 - k) \cos \theta_0$, $\cos(2\theta_0) = k^{-1} - 1/4 - \sqrt{1/16 + k^{-2}}$, $\theta_1 + 3 \theta_0 = \pi$, $k = K/J$.

(ii) In the case of strong anisotropy, only collinear (Ising) states minimize the system energy. For Mills model, independently on N , there are two discontinuous (“metamagnetic”) transitions: at $H_1 = J$ to the ferrimagnetic phase with

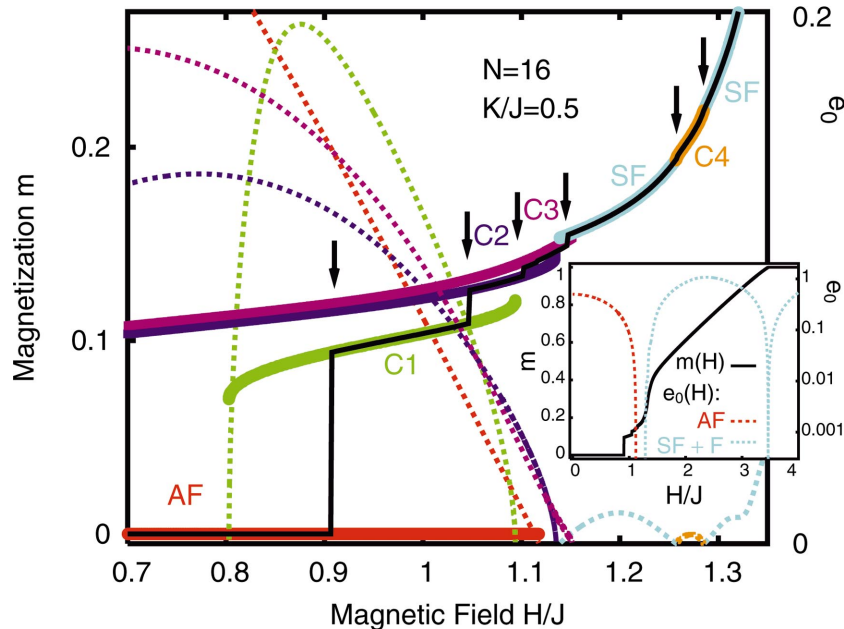


FIG. 3. (Color) Example of evolution of magnetization (continuous lines and left scales) and lowest eigenvalue of stability matrices e_0 (dotted, right scales) for Mills model ($N=16$ and $K=0.5$). Black curves: magnetization of equilibrium states, color curves for various “canted” phases C1 . . . C4 and the (reentrant) spin-flop state. Arrows mark phase transitions. Inset gives full range of field H from antiferromagnetic (AF) to ferromagnetic (F) state [half-logarithmic plot for $e_0(H)$]—details are magnified in main figure.

flipped moment at both surfaces (FM) [Fig. 1(a)], and between FM and ferromagnetic (F) phase at $H_2=2J$ (Fig. 2).

(iii) A specific inhomogeneous asymmetric *canted* (C) phase [Fig. 1(a)] arises as a transitional low symmetry structure between higher symmetry SF and FM phases. The transition FM \rightarrow C is marked by the onset of noncollinearity, i.e., a deviation of \mathbf{m}_i from the easy axis, and the transition SF \rightarrow C breaks the mirror symmetry.

The calculated phase diagram with $N=4$ in Fig. 2 includes all these phases and elucidates the corresponding magnetization processes for this Mills model. The critical points b and f at $K_b \approx 0.30$ and $K_f = \sqrt{2}$ for $N=4$ separate the phase diagram (Fig. 2) into three distinct regions. In the *low-anisotropy* region ($K < K_b$) the first-order transition from AF to the inhomogeneous SF phase occurs at the critical line $a-b$, and a further second-order transition from SF into F phase takes place at the higher field $H_f = (2 + \sqrt{2})J - K$ (dashed line $g-f$ in Fig. 2). In the *high-anisotropy* region ($K > K_f$) the above mentioned sequence of discontinuous transitions AF \rightarrow FM \rightarrow F occurs. In this region, different phases can exist as metastable states in extremely broad ranges of magnetic fields leading to severe hysteresis effects. Finally, in the intermediate region $K_b < K < K_f$ the magnetization processes have a complex character including continuous and discontinuous transitions into the C phase. For $N > 4$ the region of the C phase is subdivided into smaller areas corresponding to canted asymmetric phases separated by first-order critical lines and an area of the reentrant SF phase (Fig. 3). The number of these areas increases with increasing N . Here, the evolution of magnetic states occurs as a cascade of discontinuous transitions between different C phases.

Generally, the function (1) can be considered as the energy of a “multisublattice” antiferromagnet with N sublattices each represented by individual ferromagnetic layers. The phase diagram of such an antiferromagnet in the space of the magnetic parameters in the model (1) may include a number of new homogeneous and inhomogeneous phases and additional phase transitions. In particular, for nonequal exchange constants there is a cascade of discontinuous transitions between different ferrimagnetic phases, and exchange anisotropy K'_i may stabilize a *twisted* phase.¹⁶ Moreover, magnetic first-order transitions are accompanied by an in-

volved reconstruction of multidomain structures and hysteresis¹² which will crucially determine the magnetic properties of experimental multilayer systems. However, the basic features of the model (1) are imposed by cut exchange bonds and are revealed from Mills model. The phase diagram in Fig. 2 provides the backbone for the phase diagrams of the whole class of such nanostructures and is representative for their magnetic states.

Our results show that Mills model with finite N owns only well-defined “volume” phases and transitions between them, i.e., phases and transitions affecting the whole layer stack. The model does not include solutions for surface-confined states which were assumed to occur at a “surface spin-flop field” $H_{AF} = \sqrt{2JK + K^2}$ and to spread into the depth of the sample as the applied field increases up to the “bulk spin-flop field” $H_B = \sqrt{4JK + K^2}$.^{7,11} The critical field H_{AF} determines the stability limit of the “volume” AF phase (violet line $a-\lambda$ in Fig. 2), while the field H_B has no physical significance for the finite system. Noncollinear inhomogeneous structures similar to those discussed here as SF phase have been observed in low-anisotropic Fe/Cr superlattices.⁸ The evolution of multidomain structures accompanying spin-flop transitions was investigated in.⁹ Inhomogeneous asymmetric magnetic configurations found in Fe/Cr(211) superlattices with rather large uniaxial anisotropy^{4,7} are similar to C phases discussed in our paper. The magnetization curve Fig. 3 for Mills model with $N=16$ and $K/J=0.5$ amends similar calculations [cf. Fig. 1(a) in Ref. 4]. In addition to the transition from AF into the C phase, the above described cascade of first-order transitions between different C phases occurs. A peculiarity of $m(H)$ interpreted as the bulk spin-flop field (in Ref. 4 at $H=1.49$ kG $\hat{=} H/J=1.49$) does not correspond to a phase transition.

In conclusion, cut exchange bonds at the boundaries of antiferromagnetic superlattices cause inhomogeneous, noncollinear, or canted magnetic configurations unknown in other types of magnetic nanostructures. Experimental investigations (in particular on superlattices with small number of layers, $N=4$ and 6) should provide an interesting playground to observe the rich variety of orientational effects predicted in this paper (Fig. 2).

A. N. B. thanks H. Eschrig for support and hospitality at the IFW Dresden.

*Electronic address: u.roessler@ifw-dresden.de

[†]Permanent address: Donetsk Institute for Physics and Technology, 340114 Donetsk, Ukraine. Electronic address: bogdanov@kinetic.ac.donetsk.ua

¹P. Grünberg *et al.*, J. Appl. Phys. **61**, 3750 (1987); M. N. Baibich *et al.*, Phys. Rev. Lett. **61**, 2472 (1988); I. K. Schuller, S. Kim, and C. Leighton, J. Magn. Magn. Mater. **200**, 571 (1999).

²G. J. Strijkers, S. M. Zhou, F. Y. Yang, and C. L. Chien, Phys. Rev. B **62**, 13 896 (2000); K. Y. Kim *et al.*, J. Appl. Phys. **89**, 7612 (2001); A. Moser *et al.*, J. Phys. D **35**, R157 (2002).

³K. Ounadjela *et al.*, Phys. Rev. B **45**, 7768 (1992); S. Hamada, K. Himi, T. Okuno, and K. Takahashi, J. Magn. Magn. Mater. **240**, 539 (2002).

⁴R. W. Wang *et al.*, Phys. Rev. Lett. **72**, 920 (1994).

⁵K. Temst *et al.*, Physica B **276-278**, 684 (2000); V. V. Ustinov *et al.*, J. Magn. Magn. Mater. **226-230**, 1811 (2001).

⁶P. Steadman *et al.*, Phys. Rev. Lett. **89**, 077201 (2002).

⁷S. G. E. te Velthuis, J. S. Jiang, S. D. Bader, and G. P. Felcher, Phys. Rev. Lett. **89**, 127203 (2002).

⁸V. Lauter-Pasyuk *et al.*, Phys. Rev. Lett. **89**, 167203 (2002); V. Lauter-Pasyuk *et al.*, J. Magn. Magn. Mater. **258-259**, 382 (2003).

⁹D. L. Nagy *et al.*, Phys. Rev. Lett. **88**, 157202 (2002).

¹⁰L. Trallori *et al.*, Phys. Rev. Lett. **72**, 1925 (1994); S. Rakhmanova, D. L. Mills, and E. E. Fullerton, Phys. Rev. B **57**, 476 (1998); N. Papanicolaou, J. Phys.: Condens. Matter **10**, L131 (1998); D. L. Mills, J. Magn. Magn. Mater. **198-199**, 334 (1999); C. Micheletti, R. B. Griffiths, and J. M. Yeomans, Phys.

- Rev. B **59**, 6239 (1999); M. Momma and T. Horiguchi, *Physica A* **259**, 105 (1998).
- ¹¹D. L. Mills, *Phys. Rev. Lett.* **20**, 18 (1968); D. L. Mills and W. M. Saslow, *Phys. Rev.* **171**, 488 (1968); F. Keffer and H. Chow, *Phys. Rev. Lett.* **31**, 1061 (1973).
- ¹²A. Hubert and R. Schäfer, *Magnetic Domains* (Springer-Verlag, Berlin, 1998); V. G. Bar'yakhtar, A. N. Bogdanov, and D. A. Yablonskii, *Usp. Fiz. Nauk.* **156**, 47 (1988) [*Sov. Phys. Usp.* **31**, 810 (1988)].
- ¹³M. Alouani and H. Dreysse, *Current Opinion in Solid State Mat. Sci.* **6**, 499 (1999).
- ¹⁴S. K. Kim and J. B. Kortright, *Phys. Rev. Lett.* **86**, 1347 (2001).
- ¹⁵A. N. Bogdanov and U. K. Röbner, *Phys. Rev. Lett.* **87**, 037203 (2001); A. N. Bogdanov, U. K. Röbner, and K.-H. Müller, *J. Magn. Magn. Mater.* **238**, 155 (2002).
- ¹⁶A. N. Bogdanov and U. K. Röbner, *Phys. Rev. B* **68**, 012407 (2003).
- ¹⁷W. H. Press, S. A. Teukolsky, W. T. Vetterling, and B. P. Flannery, *Numerical Recipes in C*, 2nd ed. (Cambridge University Press, Cambridge, 1992), Chap. 10.6.
- ¹⁸F. C. Nörtemann, R. L. Stamps, A. S. Carriço, and R. E. Camley, *Phys. Rev. B* **46**, 10 847 (1992); A. L. Dantas and A. S. Carriço, *ibid.* **59**, 1223 (1999).